Environmental Earth Sciences

# EVOLUTION OF THE POLLUTION IN THE PIEDRAS RIVER NATURAL SITE (GULF OF CADIZ, SOUTHERN SPAIN) DURING THE HOLOCENE

--Manuscript Draft--

| | |
|---|---|
| **Manuscript Number:** | ENGE-D-15-01539R1 |
| **Full Title:** | EVOLUTION OF THE POLLUTION IN THE PIEDRAS RIVER NATURAL SITE (GULF OF CADIZ, SOUTHERN SPAIN) DURING THE HOLOCENE |
| **Article Type:** | Original Manuscript |
| **Corresponding Author:** | Javier Lario, Ph.D.<br>Universidad Nacional de Educacion a Distancia<br>Madrid, SPAIN |
| **Corresponding Author Secondary Information:** | |
| **Corresponding Author's Institution:** | Universidad Nacional de Educacion a Distancia |
| **Corresponding Author's Secondary Institution:** | |
| **First Author:** | Javier Lario, Ph.D. |
| **First Author Secondary Information:** | |
| **Order of Authors:** | Javier Lario, Ph.D. |
| | Jacinto Alonso-Azcárate, Ph.D. |
| | Christopher Spencer, Ph.D. |
| | Cari Zazo, Ph.D. |
| | Jose L Goy, Ph.D. |
| | Ana Cabero, Ph.D. |
| | Cristino J Dabrio, Ph.D. |
| | Francisco Borja, Ph.D. |
| | Cesar Borja, Ph.D. |
| | Jorge Civis, Ph.D. |
| | Manuel Garcia-Rodriguez, Ph.D. |
| **Order of Authors Secondary Information:** | |
| **Funding Information:** | Ministerio de Economía y Competitividad (ES)<br>(CGL2013-42847-R) — Dr. Javier Lario |
| | Ministerio de Economía y Competitividad (ES)<br>(CGL2012-33430) — Dr. Cari Zazo |
| | University of Bristol (GB) — Dr. Christopher Spencer |
| **Abstract:** | The Piedras River marshland and El Rompido spit bar is a Natural Site in close proximity to two of the most polluted rivers in the world: the Tinto and Odiel Rivers. The aim of this study is to determine the degree of contamination of this Natural Site using a variety of pollution indices. At this site the Holocene infilling sequence is recorded and applied to a study of the pollution history and the possible impacts of human activity. The depositional history of the Piedras River estuary during the Holocene recorded open marine conditions at ca. 6500 calBP when sea-level was at its Holocene maximum. To study the pollution of the estuary during the Holocene, catchment background geochemistry was established using samples that pre-date human activity (agriculture and mining). Additionally, the sedimentary environment |

| | |
|---|---|
| | was reconstructed throughout the Holocene, comparison of pollution levels is interpreted to be more reliable if the sedimentary environment has remained similar throughout the depositional record. Results show that, despite being located nearby very polluted estuaries, the Piedras River marshland contains unpolluted sediments mainly because of the small catchment area relative to that of neighbouring more polluted rivers, and thus not been affected by human activity such as mining. |
| | |

# EVOLUTION OF THE POLLUTION IN THE PIEDRAS RIVER NATURAL SITE (GULF OF CADIZ, SOUTHERN SPAIN) DURING THE HOLOCENE

J. Lario (1), J. Alonso-Azcárate (2), C. Spencer (3), C. Zazo (4), J.L. Goy (5), A. Cabero (1), C.J. Dabrio (6), F. Borja (7), C. Borja (8), J. Civis (9), M. García-Ródriguez (1)

(1) Facultad de Ciencias, Universidad Nacional de Educación a Distancia (UNED), 28040-Madrid, Spain.*

(2) Facultad de Ciencias del Medio Ambiente, Universidad de Castilla la Mancha, 45071-Toledo, Spain.

(3) Faculty of Environment and Technology, University of the West England, Bristol BS16 1QY, United Kingdom.

(4) Departamento de Geología, Museo Nacional de Ciencias Naturales-CSIC, 28006-Madrid, Spain.

(5) Departamento de Geología, Facultad de Ciencias, Universidad de Salamanca, 37008-Salamanca, Spain.

(6) Departamento de Estratigrafía & IGE (CSIC), Universidad Complutense, 28040-Madrid, Spain.

(7) Área de Geografía Física, Facultad de Humanidades, Universidad de Huelva, 21007-Huelva, Spain.

(8) Facultad de Geografía e Historia, Universidad de Sevilla, 41004-Sevilla, Spain.

(9) Instituto Geológico y Minero de España-IGME, 28003-Madrid, Spain.

* corresponding author: javier.lario@ccia.uned.es

## Abstract

The Piedras River marshland and El Rompido spit bar is a Natural Site in close proximity to two of the most polluted rivers in the world: the Tinto and Odiel Rivers. The aim of this study is to determine the degree of contamination of this Natural Site using a variety of pollution indices. At this site the Holocene infilling sequence is recorded and applied to a study of the pollution history and the possible impacts of human activity. The depositional history of the Piedras River estuary during the Holocene recorded open marine conditions at ca. 6500 calBP when sea-level was at its Holocene maximum. To study the pollution of the estuary during the Holocene, catchment background geochemistry was established using samples that pre-date human activity (agriculture and mining). Additionally, the sedimentary environment was reconstructed throughout the Holocene; comparison of pollution levels is interpreted to be more reliable if the sedimentary environment has remained similar throughout the depositional record. Results show that, despite being located nearby very polluted estuaries, the Piedras River marshland contains unpolluted sediments mainly because of the small catchment area relative to that of

neighbouring more polluted rivers, and thus has not been affected by human activity such as mining.

Keywords: Holocene sediments; Metal pollution; Heavy metals; Contamination factor; Enrichment factor; Geo-accumulation index

## 1. Introduction

The Piedras River marshland and El Rompido spit bar Natural Site is located in Huelva Province, SW Spain (Figure 1) and extends for 2,530 ha. The area was declared a Natural Site in 1989 and also a Special Area of Conservation of Wild Birds in 2002. The area has been proposed as a European Site of Community Importance. This Natural Site is located at the mouth of the Piedras River containing a tidal marshland protected from the Atlantic Ocean by a ~12 km long spit bar. This estuary is located between the Guadiana River to the west and the Tinto and Odiel Rivers to the east. These rivers drain the Iberian Pyrite Belt, the largest repository of volcanogenic massive sulphide deposits in the world, and as a result of mining within the catchment areas both rivers have high levels of pollution (Borrego et al. 2004; Delgado et al. 2009).

The geology of the drainage basin is represented in Figure 2. To the north, the Hercinian deposits are represented by Carboniferous dolomites, dolomitic limestone's and marls. Miocene deposits consist mainly of calcarenites and yellow silts while Pliocene deposits consist of grey-yellow sands and silty sand. The Quaternary deposits are represented by river terraces in the upper areas and eolian and marsh deposits in the lower areas.

The special geological characteristics of this area have led to research on the trace metals present in the sediments of the estuaries located in this area in order to evaluate the degree of contamination (Ruiz 2001; Santos Bermejo et al. 2003; Borrego et al. 2004; Lozano-Soría et al. 2005; Sainz and Ruiz 2006; Ruiz et al. 2009; Delgado et al. 2010; Carretero et al. 2011). Most of this research has been focussed on the Guadiana and Tinto-Odiel estuaries, while research in the Piedras River estuary has been less extensive and only using surface samples. Sainz

and Ruiz (2006) studied the influence of the very polluted Tinto-Odiel River and concluded that the littoral fringe extending up to 50 Km is classified as moderately to strongly polluted. Due to dominant longshore currents along this coast much of this pollution is transported to the east, some pollution is though transported to the west, reaching the mouth of the Piedras River estuary. Due to the high interest in this area as a Natural Site, the major objective of this study is to evaluate the potential heavy-metal pollution in surface and deep sediments of the marshland through the last 7000 yrs. This is the first time core samples have been recovered in order to study the pollution history of the area enabling the determination of the local background values for the heavy metals in the Piedras River estuary. In addition an attempt is made here to evaluate whether the anthropogenic activity resulting in the pollution recorded in the sedimentary record of the two adjacent river estuaries is present in the sedimentary record of the Piedras River estuary.

To study the heavy metal pollution in estuarine sediments indices such as contamination factor (CF), geoacumulation index ($I_{geo}$) and enrichment factor (EF) have been used in other coastal areas (Rubio et al. 2000; Srinivasa Reddy et al. 2004; Chen et al. 2007; Praveenna et al. 2008; Darasam et al. 2011; Feng et al. 2011) and are still used to assess contamination in soils, river environments, estuaries, lakes, reservoirs or urban sediments (Kumar et al. 2013, Zahra et al. 2014, Diop et al. 2015, Elkady et al. 2015, El-Sayed et al. 2015, Palma et al., 2015, Rivera et al. 2015, Ma et al. 2016). In order to assess sediment contamination at this location the indices cited above have been calculated with comparisons made between sediments deposited pre and post anthropogenic activity in the area. These indices have been correlated with other factors such as particle size and total organic carbon (TOC) values of the sediments.

## 2. Methodology

### 2.1. Sampling and analyses

A total of eighteen manual gouge and percussion boreholes were completed in the study area. For this study three percussion cores were selected that included a full record of the Holocene infilling sequence (cores RP-11, RP-15 and RP-16, Figure 1). These cores were sampled into

plastic pipes and stored in a fridge at -4ºC, cores were then cut longitudinally and sampled at intervals of 20 cm resulting in a total of 91 samples. Contamination was avoided by discarding the outer layer of each core section. Dates from cores were established by Lario et al. (2009) through radiocarbon dating. The ages and sedimentation rates agree with data available for others estuaries in the Gulf of Cadiz (Lario et al. 2002).

The bulk content of Cr, Cu, Ni, Pb and Zn present in the sediments was studied as they are the main heavy metals present in the area (Leblanc et al. 2000; Ruiz et al. 2008) in addition they are the trace metals typically determined in heavy metal contamination studies (Kanellopoulos et al. 2006, Feng et al. 2011). To determine the total concentration of metals in the sediment samples, 0.5g of the <63µm fraction (dry weight) obtained by dry sieving was used. The <63µm fraction was utilised as the content of heavy metals is normally accumulated in the fine fractions associated to clay minerals and oxides (Soares et al. 1999, Fan et al. 2002, Cuong and Obbard 2006). The samples were digested with a mixture of acids (9ml of concentrated HNO3 + 3ml of concentrated HCl) in Teflon® PTFE (polytetrafluoroethylene) beakers in a microwave unit (CEM MARS 5, Matthews, USA), according to EPA 3051A method (USEPA, 1996). Dissolved samples were then diluted to 40ml with milli-Q water. Following digestion, the heavy metal concentration in the sample solutions and reagent blanks was measured by ICP-AES in a Thermo iCAP 6500 spectrometer and by ICP-MS in a Thermo X-Series II spectrometer (Thermo Electron, Cambridge, UK). All reagent blanks and matrix interference were monitored throughout the analyses, and were below the instrument detection limit. The analytical method was assessed by using the 2711 Standard Reference Material (Montana Soil, from LGC Promochem, Barcelona, Spain) with an agreement of 93.3–107.7% between the certified values and the concentrations obtained by this study. Al and Fe were determined by X-ray fluorescence spectrometry, using a Phillips Spectrometer PW 1410/20 with a PW 1730 generator.

Particle size distribution was analysed by laser diffraction using a Coulter® LS 230 and Carbon content (total, organic-TOC- and inorganic-IC) of the sediments was analysed using a Shimadzu® TOC-VCSH analyser.

## 2.2. Use of pollution Indices

The metal content in sediments is the result of an addition of metals originating from natural sources and anthropogenic activity. It is estimated that the contribution of metals incorporated in sediments as a result of human causes is higher than the contribution from natural processes (Nriagu and Pacyna 1988). In a long term study such as this across the Holocene the identification of phases of raised metal concentration in sediments would typically be related with significant changes in human activities in the catchment area. Establishing the pollution history of the estuary and thus human activity in the catchment area is thus value to archaeological study of the area.

In this study, the possible sediment contamination was assessed using various pollution indices, including contamination factor and degree of contamination, index of geoaccumulation and normalized enrichment factor, these are outlined below.

***Contamination Factor (CF)***

The assessment of sediment contamination has been carried out using the contamination factor (CF) and contamination degree (CD). The approach suggested by Hakanson (1980) is applied which enables an assessment of sediment contamination through using pre-industrial levels as a reference of the background concentrations enabling comparison with post-industrial sediments.

Calculation will be simplified as:

$CF = Cm/Cb$

where *Cm* is the mean content of an individual metal in the sample and *Cb* is the pre-industrial concentration of an individual metal (background concentration). This should then identify a direct relationship between the concentration of a specific metal and how this corresponds to the background level.

Hakanson (1980) define four categories of contamination factor (CF)

CF < 1 low contamination factor

| | | |
|---|---|---|
| 1<CF<3 | moderate contamination factor |
| 3<CF<6 | considerable contamination factor |
| CF > 6 | very high contamination factor |

The contamination factor described above is a single element index. The sum of contamination factors for all elements examined represents the contamination degree (CD) of the environment and four classes are recognized (Hakanson 1980)

| | |
|---|---|
| CD < 8 | low degree of contamination |
| 8 < CD < 16 | moderate degree of contamination |
| 16 < CD < 32 | considerable degree of contamination |
| CD >32 | very high degree of contamination |

***Geo-accumulation index ($I_{geo}$)***

The geoaccumulation index ($I_{geo}$) has been used since the late 1960s, and has been widely employed in trace metal studies. Müller (1969) first used this index in basal sediments but it has also been used largely to evaluate contamination in soils (Loska et al. 2003; 2004; Yaqin et al. 2008, Rivera et al., 2015), rivers (Ma et al., 2016 ), lakes (Zahra et al., 2014, Elkady et al., 2015), beaches (Diop et al., 2015), mangroves (Praveena et al. 2008), *Ria* type embayment coasts (Rubio et al. 2000) or even harbours (Chen et al. 2007) and reservoirs (Goher et al., 2013, Palma et al., 2015). The *Igeo* enables the assessment of contamination by comparing current and pre-industrial concentrations, although it is not always easy to reach pre-industrial sediment layers (Yaqin et al., 2008). In this study, the $I_{geo}$ for selected sediments was calculated using

$I_{geo} = log_2 (Cm/1.5\ Cb)$

where *Cm* is the measured concentration of the element in the sediment and *Cb* is the geochemical background value. The constant 1.5 is used to analyse natural fluctuations in the content of a given substance in the environment and to detect very small anthropogenic influences. It is also a factor used for lithological variations of trace metals.

The geoaccumulation index consists of seven grades or classes (Müller 1979; 1981)

| | | |
|---|---|---|
| $I_{geo} < 0$ | $I_{geo}$ Class = 0 | practically uncontaminated |
| $0<I_{geo}<1$ | $I_{geo}$ Class = 1 | uncontaminated to moderate contaminated |
| $1<I_{geo}<2$ | $I_{geo}$ Class = 2 | moderate contaminated |
| $2<I_{geo}<3$ | $I_{geo}$ Class = 3 | moderate to strong contaminated |
| $3<I_{geo}<4$ | $I_{geo}$ Class = 4 | strong contaminated |
| $4<I_{geo}<5$ | $I_{geo}$ Class = 5 | strong to very strong contaminated |
| $I_{geo} > 5$ | $I_{geo}$ Class = 6 | very strong contaminated |

***Enrichment Factor (EF)***

The use of EF has been very widely applied as a means of identifying and quantifying the anthropogenic origin of certain elements since the 1970s (Chester and Stoner 1973; Duce et al. 1975), it is also a convenient measure of geochemical trends and is used for making comparisons between areas (Sinex and Helz 1981) and it is still widely used (e.g. Puig et al. 1999; Rubio et al. 2000; Karageorgis and Hatzianestis 2003; Loksa et al. 2003; 2004; Selvaraj et al. 2004; Vazquez and Sharma 2004; Kanellopoulos et al. 2006; Radakovitch et al. 2008).

The extent of metal contamination compared to the background of the catchment area was assessed using the enrichment factor (EF) (Woitke et al. 2003; Selvaraj et al. 2004). The EF was also based on the standardization of a tested element against a reference one. A reference element is the one characterized by low occurrence variability such as Sc, Mn, Ti, Al and Fe (Pacyna and Winchester 1990; Quevauviller et al. 1989; Schiff and Weisberg 1999; Reimann and De Caritat 2000; Sutherland 2000).

Some authors used Al to normalize the metals in sediments since it represents the aluminasilicates, the predominant content of coastal sediments (Chen et al. 2007, Delgado et al. 2010) but other observations support that either Al or Fe can be used for metal normalization if there is a significant correlation between them (Feng et al. 2011). Lozano-Soria et al. (2005) found a high positive correlation between Al and Fe in Piedras River sediments and thus in this study Al and Fe were used as reference elements for metal normalization.

The enrichment factor was calculated using the formula based on the equation suggested by Buat-Menard and Chesselet (1979):

$$EF = [Cm)/Cr)]/[Cmb/Crb]$$

where, *Cm* is the content of the metal in sample, *Cr* is the content of the reference element in the sample, *Cmb* is the content of the metal in the background sample and *Crb* is the content of reference element in the background sample.

In this case

$$EF_{Al} = [Cm)/C_{Al})]/[Cmb/C_{Al}b]$$

$$EF_{Fe} = [Cm)/C_{Fe})]/[Cmb/C_{Fe}b]$$

Five contamination categories are recognized on the basis of the enrichment factor (Sutherland, 2000)

| | |
|---|---|
| EF<2 | deficiency to mineral enrichment |
| 2<EF<5 | moderate enrichment |
| 5<EF<20 | significant enrichment |
| 20<EF<40 | very high enrichment |
| EF>40 | extremely high enrichment |

### 2.3. Analysis of results

A contrast independence test was carried out with the aim of determining whether significant relationships exist between variables. In addition a study of the data distribution was completed to establish the tests (parametric or non-parametric) that could be applied. A Kolmogorov-Smirnov (K-S) test was used to check the normality of the variables. Whilst Pearson Correlation Coefficient (*R*) and Spearman Correlation Coefficient (*rs*) tests were used for Normal and Non-Normal distribution, respectively. *SPSS* software was used for the calculations. This methodological approach has been applied in other geoacummulation indexes studies (Rubio et al., 2000, Diop et al., 2015).

## 3. Results and Discussion

### 3.1. Sedimentary framework

From the cores studied it is possible to interpret the Late Pleistocene and Holocene evolution of the Piedras River estuary, and thus the pollution during this period. The river is incised into coarse-grained Quaternary sediments deposited during the last major lowstand ca. 18 ka, when sea level was ~120 m lower and the coastline lay 14 km seawards from the present (Dabrio et al., 2000). Some studies of estuaries and lagoons on the coast of south-western Iberia have shown that the post-glacial transgression reached larger valleys such as the Tagus (Vis et al., 2008), Guadiana (Boski et al.,2002,2008; Delgado et al., 2012), Tinto-Odiel (Dabrio et al., 1999, 2000) and Guadalquivir (Dabrio et al.,1999, 2000) estuaries between 13,000 calBP and 10,000 calBP. Smaller valleys were only inundated when sea level reached its post-glacial maximum at about 7500-6500 calBP (Dabrio et al., 1999; Freitas et al., 2002; Schneider et al., 2010). In the Piedras River estuary the sediments underlying the Holocene estuary sequence are Miocene Pliocene (Figure 2). According to the interpretation (Lario et al., 2009) and the radiocarbon data obtained (Figure 2) the transgressed estuary basins changed from brackish to more open marine conditions as the sea rose until ca. 6500 calBP, when it reached the maximum height and the sandy estuarine barriers ceased to prograde toward the muddy central basins. Then, as it has been observed in other estuaries from the Gulf of Cadiz, rates of sedimentation and the eustatic sea-level rise decreased significantly, and the estuarine infilling was dominated by lateral progradation (Lario et al., 2002). At ca. 4000 calBP the fluvial input exceeded the rate of sea-level rise, causing partial emergence of tidal flats in the mostly filled estuarine basin. Dominance of coastal progradation upon vertical accretion at ca. 2800-2200 calBP favoured the spreading out of tidal flats and sandy barriers. Some high energy (erosional) episodes have been recorded in the upper sequence as have been interpreted in others areas of the Gulf of Cadiz (Lario et al. 2010, 2011). Also, the development of the El Rompido spit barrier during the last two centuries has partially enclosed the estuary for the first time during the Holocene.

### 3.2. Selecting geochemical background values

Through all the indices calculated, the *Cb* parameter in the equations represents the geochemical background value. The equations indicate that the index will be affected by the content of the samples and the geochemical background values.

Some authors have proposed as background reference the world average shale (Rubio et al. 2000) or the Earth's crust (Loska et al. 2003, 2004). However, these levels tend to be very general and may distort the results. Rubio et al. (2000) recommended the use of regional background values. While the geochemical background values are constant, the levels of contamination vary with time and space.

In this study, in order to evaluate the possible contamination of the area during the last 7000 yr, samples have been selected as background value samples that relate to 'natural' conditions, pre-dating the human activity. According to archaeological data, the extraction of minerals from the catchment area dates back to the age of the Iberians and Tartessos, some 5000 years ago (Davis et al. 2000; Leblanc et al. 2000; Nocete et al. 2005). Samples of that age also represent a significant point in the depositional history of the Piedras River estuary at ca. 6500 calBP, when open marine were recorded representing the Holocene sea-level maximum. Thus, samples corresponding to this age are appropriate to be used as a background level because they represent the beginning of infilling of the estuary after the maximum Holocene transgression and are unpolluted by anthropogenic activity. Importantly the environmental reconstruction identifies that the sedimentary environment has remained relatively consistent since ca. 6500 calBP, as recorded in other nearby estuaries (Lario et al. 2002), enabling reliable comparison of contamination levels through this time period.

Therefore, to estimate the background values, five samples from core RP-15 dated ca.6500 calBP were analysed and the mean values calculated. The values for the average background in the Piedras River estuary produced from this analysis were Cr: 45.8 mg/kg, Cu: 16.1 mg/kg, Ni: 27.2 mg/kg, Pb: 13.7 mg/kg and Zn: 62.2 mg/kg (Table 1).

Different background values have been calculated for the different estuaries in the south-western Spanish coast (Ruiz et al. 1998, Delgado et al. 2008; Carretero et al. 2011; Delgado et al. 2012; Table 1). All of them are based on samples of Holocene age except the one calculated

for the Tinto-Odiel estuary in which samples of Neogene and Holocene age have been used. The background values for the Tinto-Odiel estuary are slightly lower than for the other three estuaries, probably reflecting the larger time-span of samples used for the calculation. The other three estuaries show very similar background values, particularly the Doñana and Piedras River estuaries. Only the value of Cr for the Doñana estuary is significantly higher than in the other three, indicating the necessity of calculating the background values for each studied area, as local geological variations can lead to variations in the geochemistry of sediments and thus the background values among areas with similar geology.

### 3.3. Contamination Indices

A total of 91 samples from the three cores have been analysed in order to evaluate the possible record of pollution through time at the site. Particle size distribution, organic carbon content and metal concentration values are presented in Tables 2, 3 and 4. For the three cores the proportion of the clay fraction in the sample was low, generally under 10%. In cores RP-15 and RP-11 the silt fraction predominated while in RP-16 the sandy dominated. TOC values were not very high ranging between 0 and 1.76%, typically increasing towards the top of the three cores due to the organic carbon decomposition in older sediments (Kanellopoulos et al. 2006). Mean TOC values decreased along the profile towards the more marine locations in the estuary (RP-11>RP-15>RP-16, Figures 1 and 2).

For the study of the contamination indices, 14 samples have been selected (Table 5) representing different periods of time through the Holocene from the time of maximum sea-level. The samples represent the estuarine filling sequence and therefore any natural changes (e.g. flooding, increase in erosional rates…) or human induced changes (e.g. minning, farming…) during this time should be recorded. In addition, some older samples (up to ca. 9000 calBP) have been analysed in order to compare the estuarine background values with previous natural values and to detect any previous input of metals to the basin due to alluvial episodes or leaching of metallic deposits.

Table 6 shows the CF values for the selected samples. All values were in the *low contamination factor* or low values *of moderate contamination factor* categories. Therefore, all samples showed a low degree of contamination except for the surface samples, which showed a moderate degree of contamination.

The $I_{geo}$ (Table 7) shows the same tendency as the CF index with uncontaminated levels in most samples. $I_{geo}$ values are lower than 1, which classifies the sediments as unpolluted, similar to the values calculated by Ruiz (2001) in surface samples. The enrichment factors ($EF_{Al}$ and $EF_{Fe}$, Table 8) both showed similar trends and most samples indicate deficiency to mineral enrichment.

### 3.4. Statistical Analysis

Tables 9, 10, and 11 shows the Pearson correlation matrix for the particle size fractions, TOC and the heavy metals studied. It can be seen that both the grain size and total organic carbon are important factors affecting the metal distribution in the sediments with high correlation factors. Generally there is a strong correlation between the quantity of the fine fractions and trace metal concentrations (Wang and Chen 2000; Huang and Lin 2003) while in this study the TOC values were relatively more important than grain size in controlling the distribution of trace metals in the sediments as it correlates with higher values with all metals than with the clay content. These results demonstrate that organic matter content was a more important factor affecting the trace metal concentrations than the grain size distribution. The Cr, Ni, Pb, Zn and Cu correlate positively for all the sections, which indicate a common geogenic origin for the assemblage.

TOC has a positive correlation with clay and silt fractions and negative with the sand fraction (Tables 9, 10 and 11) which indicates that organic matter in the sediments was fine to very fine grained.

The study of all the contamination indices clearly shows a consistent trend indicating that the Piedras River estuary sediments display no signs of contamination as a result of human activity during the Holocene. This greatly contrasts with the situation of the adjacent estuaries.

The Iberian Pyrite Belt (IPB), with over 1,600 million tons of polymetallic massive sulphide deposits originally in place and about 2,500 million tons of mineralization in the stockwork, is one of the most significant metallogenic areas in the world and possibly the largest concentration of sulphides worldwide. Also, the Iberian Pyrite Belt is one of the oldest mining districts in the world with mining activity recorded over the last 5000 years. Mining commenced in the Chalcolithic period (3rd millennium BC) and continued during the Bronze Age and Tartessian civilization. During Roman times industrial mining extracted more than 20 million tons. After the abandonment of the mines in the 4th century BC, the mines were exploited only on a minor scale. In the late nineteenth century the mining was operated by British and French companies, and large-scale, open-pit operations prevailed until the deposits had been essentially depleted about a century later. Due to this activity the Tinto and Odiel Rivers represent an extreme case of acid mine drainage with high concentrations of toxic elements. The many sources of pollution, along with the low buffering capacity of the rocks that form the substrate of the basins of the Tinto and Odiel Rivers, result in high levels of contamination, unparalleled worldwide. (Ruiz 2001; Sainz and Ruiz 2006; Olias and Nieto 2012).

In the Doñana estuary relatively polluted sediments (3800-3000 calBP) have been found derived from old mining activities located in its catchment area (Carretero et al. 2011). In the Guadiana estuary Delgado et al. (2012) determined background levels from core sediments unaffected by human activities and determined that the surface elements of the estuary with ages younger than 4500 calBP contain significant levels of contamination associated with the mining activities in the IPB. Firstly the Guadiana Estuary sediments record a general increase in elements such as Co, Cr and Ni in the Copper Age, in the Bronze age and in the Roman period greater increases of heavy metals were recorded. Finally the most recent period of modern mining activities are also recorded in the heavy metal contents of the estuary sediments.

The absence of pollution in Piedras River estuary is interpreted as being due to the fact that in the Piedras River catchment area there are no mineral ore deposits and thus no historic mining activity. Sainz and Ruiz (2006) found that the presence of pollution at the mouth of the Piedras River indicates the influence of flow from the Tinto and Odiel Rivers. Absence of this pollution in

the estuarine sediments indicate than the inner estuary has not been influenced by discharge from the Tinto and Odiel Rivers during the Holocene and, therefore, the dominant longshore currents in this area have remained the same (towards the east) throughout the Holocene. There is no evidence of the transfer of contaminants between the closed basins by wind or by the sea, and thus sedimentation in the Piedras River is dominated by fluvial input rather than from extra-estuary marine sources.

Data obtained in this study supports that of studies of surficial pollution in the Piedras River estuary (Ruiz 2001; Lozano-Soria et al. 2005), that found very low or unpolluted sediment. Furthermore we found that this characteristic extends throughout the last 7000 yr confirming that the area has not been influenced by pollution from human activity during the Holocene. Whilst similarities exist between this study and the previous studies in the region it must be stressed that previous work was limited to surficial samples and used background values from the nearby Tinto-Odiel estuary. Therefore, this study represents the first investigation where the research has included the study of the entire estuarine sequence and has used local geochemical background values in order to evaluate the record of the trace metals in the estuary trough the time.

## Conclusions

This study evaluated the degree of heavy-metal contamination of the Piedras River Natural Site using a variety of pollution indices. Through analysing sediments derived from deep coring it has been possible to recover the entire Holocene sedimentary sequence of the estuary and for the first time local geochemical background values of uncontaminated sediments has been established.

The comparison of background geochemical values from different estuaries in the area reveals the necessity of calculating the background values for an estuary using local data and an adequate time-span. Local geological variations can result in key changes in the geochemistry of sediments producing changes in the background values among areas with similar geology.

For the first time in the Piedras River estuary this work uses the study of the entire estuarine sequence and local geochemical background data, in order to evaluate the evolution of the trace metals in the estuary trough the time. Pollution indices reveal low or unpolluted sediments, extending through the last 7000 yr, and confirming that the area has not been influenced by pollution from human activity during the Holocene. The results presented here agree with previous work on this estuary that was limited to surficial samples, and using regional background values (from the nearby Tinto-Odiel estuary, Ruiz 2001; Lozano-Soria et al. 2005). Results show that all of the pollution indices calculated dismiss any trace of heavy-metal pollution through the last 7000 years and therefore there is no evidence of any minning activity in this catchment area. The heavy-metal concentrations are of geogenic origin and appear to be linked to the amount of fine grained organic matter in the sediments rather to clay fraction. The results also indicate that the estuary has not been influenced by extra-estuary pollution sources from the nearby polluted Guadalquivir Rivers, Guadiana River or Tinto and Odiel Rivers. It can also be inferred that the dominant longshore currents in this area have remained the same during the Holocene and that sedimentation in the Piedras River estuary is dominated by fluvial input rather that extra-estuary marine sources. This study provides new pollution data and detail of estuary evolution during Holocene; such details are relevant for the preservation of this Natural Site and Special Area of Conservation of Wild Birds.

**Acknowledgements:**

This paper has been funded by research projects CGL2012-33430 and CGL2013-42847-R and also funding from the Faculty of Environment and Technology, UWE Bristol.

**References:**

Buat-Menard, P., Chesselet, R. 1979. Variable influence of the atmospheric flux on the trace metal chemistry of oceanic suspended matter. Earth Planet. Sci. Lett. 42: 398-411.

Borrego, J.; López-Gonzalez, N.; Carro, B. 2004. Geochemical signature as paleoenvironmental markers in Holocene sediments of the Tinto River estuary (Southwestern Spain). Estuarine, Coastal and Shelf Science 61: 631-641.

Boski, T., Moura, D., Veiga-Pires, C., Camacho ,S., Duarte, D., Scott, D.B., Fernandes, S.G. 2002. Postglacial sea-level rise and sedimentary response in the Guadiana Estuary, Portugal/Spain border. Sedimentary Geology 150: 103-122.

Boski, T., Camacho, S., Moura, D., Fletcher, W., Wilamowski, A., Veiga-Pires, C., Correia, V., ,Loureiro, C., Santana,P. 2008. Chronology of the sedimentary processes during the postglacial sea level rise in two estuaries of the Algarve coast, Southern Portugal. Estuarine, Coastal and Shelf Sciences 77: 230-244.

Carretero, M.I., Pozo, M., Ruiz, F., Rodríguez-Vidal, J., Cáceres, L.M., Abad, M., Muñoz, J.M., Gómez, F., Campos, J.M., González-Regalado, M.L., Olías, M. 2011. Trace elements in Holocene sediments of the southern Doñana National Park (SW Spain): historical pollution and applications. Environ. Earth Sci. 64: 1215-1223.

Chen, C., Kao, C. Chen, CF., Dong, C. 2007. Distribution and accumulation of heavy metals in the sediments of Kaohsiung Harbor, Taiwan. Chemosphere 66: 1431-1440.

Chester, R., Stoner, J.H. 1973. Pb in particulates from lower atmosphere of the eastern Atlantic. Nature 245: 27-28.

Cuong D.T., Obbard, J.P. 2006. Metal speciation in coastal marine sediments from Singapore using a modified BCR-sequential extraction procedure. Appl. Geochem. 21: 1335-1346.

Dabrio, C.J.; Zazo, C.; Lario, J.; Goy, J.L.; Sierro, F.J.; Borja, F.; González, J.A.; Flores, J.A. 1999. Sequence stratigraphy of Holocene incised-valley fills and coastal evolution in the Gulf of Cadiz (southern Spain). Geologie en Minjbow 77: 263-281.

Dabrio, C.J.; Zazo, C.; Goy, J.L.; Sierro, F.; Borja, F.; Lario, J.; González, J.A.; Flores, J.A. 2000. Depositional history of estuarine infill during the Late Pleistocene-Holocene postglacial transgression. Marine Geology, 162: 381-404.

Dasaram, B., Satyanarayanan, M., Sudarshan, V., Keshav Krishna, A. 2011. Assessment of Soil Contamination in Patancheru Industrial Area, Hyderabad, Andhra Pradesh, India. Research Journal of Environmental and Earth Sciences 3: 214-220.

Davis, R.A., Welty, A.T., Borrego, J., Morales, J.A., Pendón, J.G., Ryan, J.G. 2000. Rio Tinto estuary (Spain): 5000 years of pollution. Environmental Geology 39: 1107-1116.

Delgado, J., Nieto, J.M., Boski, T., Alabardeiro, L. 2008. Determinación de los valores de fondo regional en sedimentos Holocenos del estuario del río Guadiana (SW de España). Geogaceta 44: 235-238.

Delgado, J., Sarmiento, A., Condesso de Melo, M., Nieto, J. 2009. Environmental impact of mining activities in the southern Sector of the Guadiana basin (SW of the Iberian Peninsula). Water, Air, and Soil Pollution 199: 323-341.

Delgado, J., Nieto, J.M., Boski, T. 2010. Analysis of the spatial variation of heavy metals in the Guadiana Estuary sediments (SW Iberian Peninsula) based on GIS mapping techniques. Estuarine. Coastal and Shelf Science 88: 71-83.

Delgado, J., Boski, T., Nieto, J.M., Pereira, L., Moura, D., Gomes, A., Sousa, C., García-Tenorio, R. 2012. Sea-level rise and anthropogenic activities recorded in the late Pleistocene/Holocene sedimentary infill of the Guadiana Estuary (SW Iberia). Quarter. Sci. Rev. 33: 121-141.

Diop, C., Dewaelé, D., Cazier, F., Diouf, A., Ouddane, B. 2015. Assessment of trace metals contamination level, bioavailability and toxicity in sediments from Dakar coast and Saint Louis estuary in Senegal, West Africa. Chemosphere 138: 980-987.

Duce, R. A., Hoffmann, G. L., Zoller, W. H. 1975. Atmospheric trace metals at remote northern and southern hemisphere sites: Pollution or natural?. Science, 187: 59-61.

Elkady, A.A., Sweet, S.T., Wade, T.L., Klein, A.G. 2015. Distribution and assessment of heavy metals in the aquatic environment of Lake Manzala, Egypt. Ecological Indicators 58: 445-457.

El-Sayed, S.A., Moussa, E.M.M., El-Sabagh, M.E.I. 2015. Evaluation of heavy metal content in Qaroun Lake, El-Fayoum, Egypt. Part I: Bottom sediments. Journal of Radiation Research and Applied Sciences 8: 276-285.

Fan,W.H., Wang,W.X., Chen, J.S., LI,X.D., Yen, Y.F. 2002. Cu, Ni, and Pb speciation in surface sediments from a contaminated bay of northern China. Mar. Pollu. Bull. 44: 820-826.

Feng, H., Jiang, H., Gao, W., Weinstein, M.P., Zhang, Q., Zhang, W., Yu, L., Yuan, D., Tao, J. 2011. Metal contamination in sediments of the western Bohai Bay and adjacent estuaries, China. J. Environ. Manage. 92: 1185-1197.

Freitas, M.C., Andrade, C., Cruces, A., 2002. The geological record of environmental changes in southwestern Portuguese coastal lagoons since the Lateglacial. Quaternary International 93-94: 161-170.

Goher, M.E., Farhat, H.I., Abdo, M.H., Salem, S.G., 2014. Metal pollution assessment in the surface sediment of Lake Nasser, Egypt. J. Aquat. Res. 40: 213–224.

Hakanson, L. 1980. An ecological risk index for aquatic pollution control. A sedimentological approach. Water Res., 14: 975-1001.

Huang, K.M., Lin, S. 2003. Consequences and implications of heavy metal spatial variations in sediments of the Keelung River drainage basin, Taiwan. Chemosphere 53: 1113-1121.

Kanallopoulos, T.D.; Angelidis, M.O.; Karageorgis, A.P.; Kaberi, H.; Kapsimalis, V.; Anagnostuo, C. 2006. Geochemical composition of the uppermost prodelta sediments of the Evros River, northeastern Aegean Sea. Journal of Marine Systems 63: 63-78.

Karageorgis, A. P., Hatzianestis, I. 2003. Surface sediment chemistry in the Olympic Games 2004 Sailing Center (SaronikosGulf). Mediterranean Marine Science 4: 5–22.

Kumar, A., Yadav, S., Kumar, P., Kumar, R. 2013. Source apportionment and spatial–temporal variations in the metal content of surface dust collected from an industrial area adjoining Delhi, India. Science of the Total Environment 443: 662-672.

Lario, J.; Zazo, C.; Goy, J.L.; Dabrio, C.J.; Borja, F.; Silva, P.G.; Sierro, F.; Gonzalez, F.; Soler, V.; Yll, R. 2002. Changes in sedimentation trends in SW Iberia Holocene estuaries. Quaternary International 93-94: 171-176.

Lario, J.; Zazo, C.; Goy, J.L.; Cabero, A.; Bardaji, T.; Dabrio, C.J.; Borja, F.; Civis, J.; Borja, C.; Spencer, C.; Alonso-Azcarate, J. 2009. Estuarine infill after the last postglacial transgression in Rio Piedras marshland (Gulf of Cádiz, Southern Spain). In: Quaternary Land-Ocean Interactions: Driving mechanisms and coastal responses. IGCP 495 Annual Conference, South Carolina, USA, pp. 56-57.

Lario, J., Luque, L., Zazo, C. Goy, J.L., Spencer, C., Cabero, A., Bardají, T., Borja, F., Dabrio, C.J., Civis, J., González-Delgado, J.A., Borja, C., Alonso-Azcárate, J. 2010. Tsunami vs. Storm surge deposits: a review of the sedimentological and geomorphological records of extreme wave events (EWE) during the Holocene in the Gulf of Cadiz, Spain. Z. Geomorph. 54, Suppl.3 301-316.

Lario, J., Zazo, C., Goy, J.L., Silva, P.G., Bardají, T., Cabero, A., Dabrio, C.J. 2011. Holocene paleotsunami catalogue of SW Iberia. Quaternary International 242: 196-200.

Leblanc, M.; Morales, J.A.; Borrego, J.; Elbaz-Poulichet, F. 2000. 4,500 year-old mining pollution in southwestern Spain: long term implications for modern mining pollution. Econ. Geol. 95: 655-662.

Loska, K., Wiechula, D., Barska, B., Cebula, E., Chojnecka, A. 2003. Assessment of Arsenic enrichment of cultivated soils in Southern Poland. Polish Journal of Environmental Studies 2: 187-192.

Loska, K., Wiechula, D., Korus, I. 2004. Metal contamination of farming soils affected by industry. Environ. Inter. 30: 159-165.

Lozano-Soria, O., Borrego,J., López-González, N., Carro, B. 2005. Características geoquímicas y factores de enriquecimiento (FE) de los sedimentos estuarinos de la Costa de Huelva (SW España). Geogaceta 38: 147-150.

Ma, X., Zuo, H., Tian, M., Zhang, L., Meng, J., Zhou, X., Min, N., Chang, X., Liu, Y. 2016. Assessment of heavy metals contamination in sediments from threeadjacent regions of the Yellow River using metal chemical fractions and multivariate analysis techniques. Chemosphere 144: 264-272.

Müller, G. 1969. Index of geoaccumulation in sediments of the Rhine River. Geojournal 2: 108-118.

Müller, G. 1979. Schwermetalle in den sediments des Rheins-Veranderungen seitt 1971. Umschan 79: 778-783.

Müller, G. 1981. The heavy metal pollution of the sediments of Neckars and its tributary: A stocktaking. Chem. Zeit. 105: 157-164.

Nocete, F., Álex, E., Nieto, J.M., Sáez, R., Inácio, N., Bayona, M.R. 2005. Intensidad e intensificación en la primera minería y metalurgia del cobre especializada de la Península Ibérica (III milenio ane): la identificación arqueológica de un proceso regional de deforestación y polución. Revista Atlántica-Mediterránea de Prehistoria y Arqueología Social 7: 33-49.

Nriagu, J.O., Pacyna, J.M. 1988. Quantitative assessment of worldwide contamination of air, water and soils by trace metals. Nature 333:134-139.

Olías, M., Nieto, J.M. 2012. El impacto de la minería en los ríos Tinto y Odiel a lo largo de la historia. Rev. Soc. Geol.España 25:177-192.

Pacyna, J.M., Winchester, J.W. 1990. Contamination of the global environment as observed in the Arctic. Palaeogeogr Palaeoclimatol Palaeoecol. 82: 149-57.

Palma, P., Ledo, L., Alvarenga, P. 2015. Assessment of trace element pollution and its environmental risk to freshwater sediments influenced by anthropogenic contributions: The case study of Alqueva reservoir (Guadiana Basin). Catena 128: 174-184.

Praveena, S.M., Ahmed, A., Radojevic, M., Abdullah, M.H., Aris, A.Z. 2008. Multivariate and Geoaccumulation Index Evaluation in Mangrove Surface Sediment of Mengkabong Lagoon, Sabah. Bull Environ Contam Toxicol. 81: 52-56.

Puig, P., Palanques, A., Sánchez-Cabeza, J. A., Masque, P. 1999. Heavy metals in particulate matter and sediments in the southern Barcelona sedimentation system (northwestern Mediterranean). Marine Chemistry, 63: 311-329.

Quevauviller, P., Lavigne, R., Cortez, L. 1989. Impact of industrial and mine drainage wastes on the heavy metal distribution in the drainage basin and estuary of the Sado River (Portugal). Environ Pollut. 59: 267- 286.

Radakovitch, O., Roussiez, V., Ollivier, P., Ludwig,W., Grenz, C., Probst, J. L. 2008. Input of particulate heavy metals from rivers and associated sedimentary deposits on the Gulf of Lion continental shelf. Estuar Coast Shelf Sci. 77: 285-295.

Reimann, C., De Caritat, P. 2000. Intrinsic flaws of element enrichment factors (EFs) in environmental geochemistry. Environ. Sci. Technol. 34: 5084-5091.

Rivera M.B., Fernández-Caliani, J.C., Giráldez, M.I. 2015. Geoavailability of lithogenic trace elements of environmental concern and supergene enrichment in soils of the Sierra de Aracena Natural Park (SW Spain). Geoderma 259-260:164-173.

Rubio, B., Nombela, M.A., Vilas, F. 2000. Geochemistry of major and trace elements in sediments of the Ria de Vigo (NW Spain): an assessment of metal pollution. Mar. Pollut. Bull. 40: 968-980.

Ruiz, F., Gonzalez-Regalado, M.L., Borrego, J., Morales, J.A., Pendón, J.G., Muñoz, J.M. 1998. Stratigraphic sequence, elemental concentrations and heavy metal pollution in Holocene sediments from the Tinto-Odiel Estuary, southwestern Spain. Environmental Geology 34: 270-278.

Ruiz, F. 2001. Trace metals in estuarine sediments from the southwestern Spanish coast. Mar. Pollut. Bull. 42: 481-489.

Ruiz, F., Borrego, J., González-Regalado, M.L., López-González, N., Carro, B., Abad, M. 2008. Impact of millennial mining activities on sediments and microfauna of the Tinto River estuary (SW Spain). Marine Pollution Bulletin 56: 1258-1264.

Ruiz, F., Borrego, J., González-Regalado, M.L., López-González, N., Carro, B., Abad, M. 2009. Interaction between sedimentary processes, historical pollution and microfauna in the Tinto Estuary (SW Spain). Environmental Geology 58: 779-783.

Sainz, A., Ruiz, F. 2006. Influence of the very polluted inputs of the Tinto-Odiel system on the adjacent litoral sediments of southwestern Spain: a statistical approach. Chemosphere 62: 1612-1622.

Santos Bermejo, J.C., Beltrán, R., Gómez Ariza, J.L. 2003. Spatial variations of heavy metals contamination in sediments from Odiel river (Southwest Spain). Environment International 29: 69-77.

Schiff, K.C., Weisberg, S. 1999. Iron as a reference element for determining trace metal enrichement in California coastal shelf sediments. Mar Environ Res. 48: 161-179.

Schneider, H., Hofer, D., Trog, C., Busch, S., Schneider, M., Baade, J., Daut, G., Mausbacher, R. 2010. Holocene estuary development in the Algarve Region (Southern Portugal) - a reconstruction of sedimentological and ecological evolution. Quaternary International 221: 141-158.

Selvaraj, K., Ram Mohan, V., Szefer, P. 2004. Evaluation of metal contamination in coastal sediments of the Bay of Bengal, India: geochemical and statistical approaches. Mar. Pollut. Bull. 49: 174-185.

Sinex, S.A., Helz, G.R. 1981. Regional geochemistry of trace elements in Chesapeake Bay sediments. Environmental Geology 3: 315-323.

Srinivasa Reddy, Shaik Basha, Sravan Kumar, V.G., Joshi, H.V., Ramachandraiah, G. 2004. Distribution, enrichment and accumulation of heavy metals in coastal sediments of Alang–Sosiya ship scrapping yard, India. Marine Pollution Bulletin 48: 1055-1059.

Soares, H.M.V.M., Boaventura, R.A.R., Machado, A.A.S.C., Da Silva, J.C.G.E. 1999. Sediments as monitors of heavy metal contamination in the Ave river basin (Portugal): multivariate analysis of data. Environ. Poll. 105: 311-323.

Sutherland, R.A. 2000. Bed sediments associated trace metals in an urban stream, Oahu, Hawaii. Environ. Geol. 39: 611-627.

USEPA. 1996. Microwave Assisted Acid Digestion of Sediments, Sludges, Soils and Oils, Method 3051A. USEPA, Washington, DC, USA.

Vazquez, F. G., Sharma, V. K. 2004. Major and trace elements in sediments of the Campeche Sound, southeast Gulf of Mexico. Mar. Poll. Bull. 48: 87-90.

Wang, F., Chen, J.: 2000. Relation of sediment characteristics to trace metal concentrations: a statistical study. Wat. Res. 34: 694-698.

Woitke, P., Wellmitz, J., Helm, D., Kube, P., Lepom, P., Litheraty, P.: 2003. Analysis and assessment of heavy metal pollution in suspended solids and sediments of the river Danube. Chemosphere 51: 633-642.

Yaqin, J., Yinchang, F., Jianhui, W., Tan, Z., Zhipeng, B.; Chiqing, D. 2008. Using geoaccumulation index to study source profiles of soil dust in China. Journal of Environmental Sciences 20: 571-578.

Zahra, A. Hashmi, M.Z.; Malik, R.N., Ahmed, Z. 2014. Enrichment and geo-accumulation of heavy metals and risk assessment of sediments of the Kurang Nallah-Feeding tributary of the Rawal Lake Reservoir, Pakistan. Science of the Total Environment 470-471: 925-933.

Figures caption:

Figure 1. Location of the study area and cores.

Figure 2. Geological map of the study area.

Figure 3. Sedimentology of the cores and cross section, with indication of the Holocene estuary sequence studied.

Figure1

Click here to download Figure Figure 1.jpg

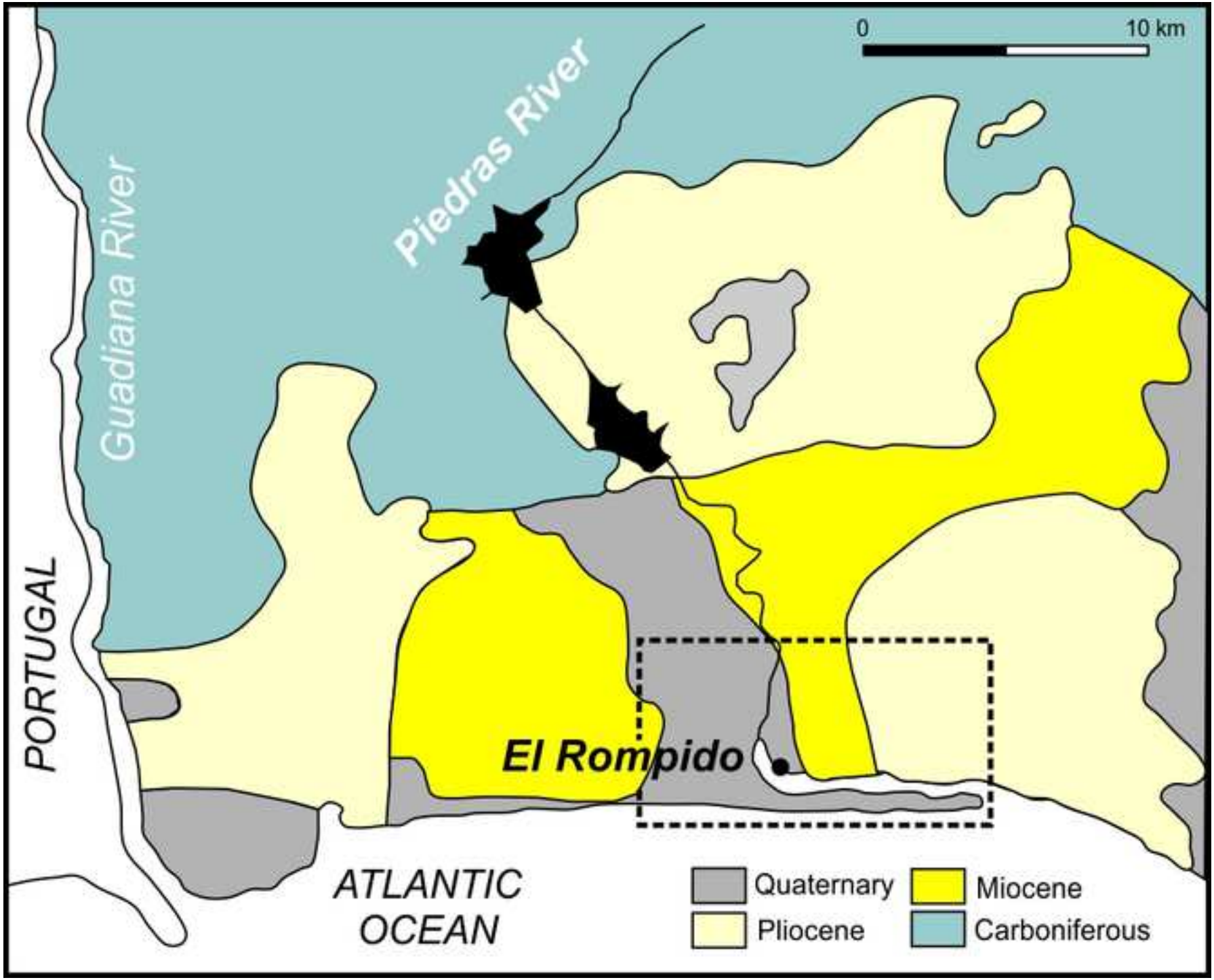

Figure2

Click here to download Figure Figure 2.jpg

Figure3

Click here to download Figure Figure 3.jpg

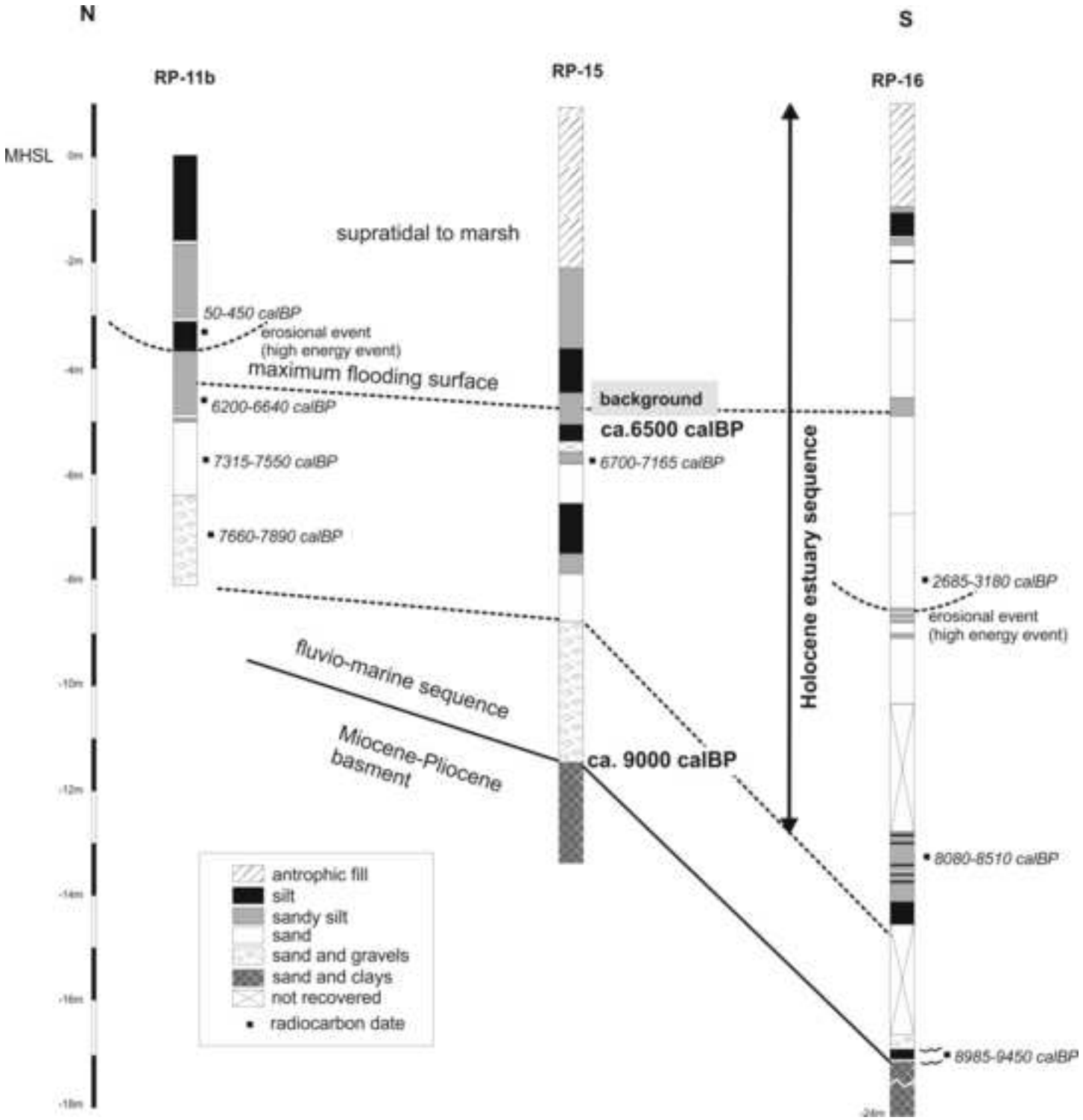

Table 1. Background geochemical values calculated in the different estuaries of the Southwestern Spanish Coast (element concentrations in mg/Kg).

| Estuary | Cr | Cu | Ni | Pb | Zn |
|---|---|---|---|---|---|
| Tinto-Odiel[1] | 21.1 | 13.0 | 12.4 | 15.4 | 39.0 |
| Guadiana[2] | 23.4 | 28.0 | 32.6 | 19.7 | 76.4 |
| Doñana[3] | 69.6 | 19.0 | 27.2 | 12.6 | 62.2 |
| Piedras (this work) | 45.8 | 16.1 | 27.2 | 13.7 | 62.2 |

[1] Ruiz et al., 1998, [2] Delgado et al., 2012, [3] Carretero et al, 2011

Table 2. Particle size distribution, organic carbon content and metal concentration values in RP-11b core. (mbsl: metres below sea level. Element concentrations in mg/Kg).

| mbsl | % Sand | % Silt | % Clay | TOC | Cr | Cu | Ni | Pb | Zn | $Al_2O_3$ | $Fe_2O_3$ |
|---|---|---|---|---|---|---|---|---|---|---|---|
| 0.10 | 61.06 | 34.28 | 4.66 | 1.49 | 37.55 | 19.33 | 25.8 | 17.22 | 69.63 | 161506 | 45986 |
| 0.29 | 52.21 | 40.28 | 7.51 | 0.82 | 45.05 | 23.72 | 31.28 | 27.98 | 92.05 | 190818 | 55534 |
| 0.50 | 16.59 | 73.33 | 10.08 | 1.12 | 58.95 | 25.58 | 31.95 | 25.39 | 119.17 | 189343 | 44251 |
| 0.69 | 31.22 | 57.64 | 11.13 | 1.7 | 49.99 | 21.34 | 27.6 | 8.24 | 52.76 | 170146 | 42832 |
| 0.89 | 22.42 | 69.89 | 7.69 | 1.53 | 47.97 | 17.19 | 31.3 | 13.59 | 67.83 | 192775 | 53833 |
| 1.09 | 29.86 | 64.13 | 6.02 | 1.66 | 55.24 | 17.38 | 31.85 | 13.96 | 73.55 | 192871 | 50667 |
| 1.28 | 36.21 | 58.53 | 5.26 | 1.66 | 53.92 | 18.64 | 31.18 | 18.35 | 66.65 | 184790 | 52880 |
| 1.49 | 31.22 | 56.92 | 11.86 | 1.29 | 55.62 | 18.00 | 30.81 | 15.24 | 68.61 | 197444 | 49894 |
| 1.65 | 25.27 | 66.33 | 8.39 | 1.31 | 52.74 | 20.23 | 32.47 | 15.9 | 72.75 | 189187 | 63720 |
| 1.89 | 34.78 | 58.19 | 7.04 | 1.17 | 45.84 | 19.15 | 29.8 | 21.22 | 73.14 | 182385 | 52251 |
| 2.09 | 47.62 | 46.99 | 5.39 | 1.53 | 61.09 | 20.38 | 34.16 | 18.90 | 79.98 | 192762 | 53319 |
| 2.29 | 14.75 | 76.77 | 8.48 | 1.20 | 51.42 | 19.65 | 30.19 | 16.09 | 72.53 | 197418 | 52888 |
| 2.49 | 34.19 | 61.20 | 4.61 | 1.70 | 54.32 | 17.12 | 29.17 | 13.21 | 65.54 | 185522 | 52702 |
| 2.69 | 28.04 | 71.96 | 0.00 | 1.45 | 50.06 | 20.03 | 30.75 | 15.10 | 71.53 | 188733 | 50499 |
| 2.89 | 37.42 | 56.20 | 6.38 | 0.97 | 50.82 | 18.17 | 29.47 | 13.64 | 65.56 | 188246 | 49440 |
| 3.09 | 53.18 | 41.79 | 5.03 | 0.87 | 44.63 | 17.13 | 28.52 | 14.33 | 60.86 | 165662 | 44644 |
| 3.29 | 35.18 | 57.45 | 7.37 | 1.43 | 48.55 | 20.71 | 35.11 | 20.54 | 69.98 | 182468 | 53106 |
| 3.49 | 35.53 | 57.33 | 7.14 | 1.64 | 45.11 | 17.33 | 29.71 | 14.68 | 68.36 | 186184 | 54879 |
| 3.69 | 54.64 | 40.73 | 4.63 | 1.76 | 43.97 | 17.63 | 28.65 | 14.54 | 69.07 | 177240 | 52858 |
| 3.89 | 30.46 | 61.78 | 7.76 | 1.29 | 53.24 | 19.23 | 31.24 | 15.44 | 67.21 | 189073 | 50774 |
| 4.09 | 30.97 | 61.92 | 7.11 | 1.03 | 53.73 | 19.35 | 32.65 | 15.41 | 68.52 | 187531 | 49340 |
| 4.29 | 27.62 | 65.11 | 7.26 | 1.22 | 54.17 | 18.37 | 30.41 | 14.30 | 66.86 | 155523 | 48899 |
| 4.49 | 54.45 | 41.05 | 4.50 | 1.11 | 55.17 | 16.54 | 30.09 | 14.85 | 59.87 | 188105 | 50943 |
| 4.69 | 52.72 | 42.08 | 5.20 | 0.99 | 51.04 | 17.63 | 30.66 | 14.23 | 65.84 | 182065 | 45736 |
| 4.89 | 49.88 | 45.68 | 4.45 | 1.09 | 57.62 | 17.69 | 32.44 | 15.61 | 63.00 | 186608 | 64058 |
| 5.09 | 28.97 | 60.86 | 10.17 | 0.60 | 55.87 | 17.16 | 31.77 | 15.63 | 60.99 | 162571 | 48540 |
| 5.28 | 77.37 | 19.32 | 3.31 | 0.12 | 45.57 | 16.15 | 25.16 | 14.00 | 51.43 | 98949 | 22145 |
| 5.48 | 71.53 | 23.81 | 4.66 | 0.08 | 39.44 | 12.99 | 23.6 | 11.30 | 47.00 | 76949 | 15868 |
| 5.60 | 74.58 | 20.94 | 4.49 | 0.04 | 37.61 | 15.09 | 21.28 | 11.98 | 46.39 | 88591 | 17805 |
| 5.79 | 87.54 | 9.76 | 2.70 | 0.02 | 30.74 | 9.44 | 18.38 | 8.48 | 37.59 | 73571 | 14587 |
| 6.00 | 91.45 | 6.91 | 1.63 | 0.03 | 34.52 | 10.67 | 20.23 | 9.34 | 43.96 | 86234 | 15905 |
| 6.20 | 87.03 | 11.33 | 1.63 | 0.16 | 33.44 | 13.58 | 26.49 | 10.41 | 43.53 | 95478 | 21936 |

Table 3. Particle size distribution, organic carbon content and metal concentration values in RP-15 core. (mbsl: metres below sea level. Element concentrations in mg/Kg)

| mbsl | % Sand | % Silt | % Clay | TOC | Cr | Cu | Ni | Pb | Zn | $Al_2O_3$ | $Fe_2O_3$ |
|---|---|---|---|---|---|---|---|---|---|---|---|
| 3.70 | 32.90 | 60.19 | 6.91 | 1.09 | 47.67 | 15.93 | 27.22 | 13.77 | 66.81 | 177806 | 50918 |
| 3.89 | 34.81 | 58.16 | 7.03 | 0.98 | 51.04 | 15.22 | 28.25 | 14.76 | 65.69 | 176185 | 40688 |
| 4.09 | 35.25 | 58.00 | 6.74 | 1.01 | 45.06 | 13.94 | 26.15 | 13.36 | 57.04 | 173337 | 44966 |
| 4.29 | 29.56 | 61.20 | 9.24 | 1.19 | 47.50 | 18.02 | 29.35 | 14.17 | 66.47 | 169573 | 58714 |
| 4.54 | 42.19 | 51.29 | 6.52 | 1.02 | 53.18 | 17.36 | 30.2 | 15.34 | 67.16 | 159252 | 47971 |
| 4.69 | 39.50 | 53.39 | 7.11 | 0.98 | 41.57 | 15.69 | 26.09 | 14.87 | 68.04 | 170923 | 45714 |
| 4.93 | 21.61 | 68.64 | 9.75 | 0.95 | 40.10 | 16.06 | 26.65 | 13.47 | 57.52 | 168593 | 50820 |
| 5.09 | 22.77 | 69.06 | 8.17 | 0.98 | 47.77 | 16.04 | 28.19 | 13.2 | 61.69 | 183076 | 52808 |
| 5.29 | 24.89 | 67.44 | 7.67 | 1.05 | 44.01 | 15.04 | 26.11 | 12.98 | 62.59 | 175093 | 48227 |
| 5.49 | 20.91 | 71.72 | 7.37 | 0.91 | 41.88 | 15.54 | 25.94 | 13.17 | 57.59 | 169596 | 49042 |
| 5.69 | 16.14 | 75.07 | 8.79 | 0.99 | 40.05 | 12.81 | 23.51 | 12.50 | 52.15 | 164926 | 50526 |
| 5.90 | 33.59 | 59.32 | 7.09 | 1.03 | 47.49 | 16.66 | 27.30 | 14.20 | 67.06 | 167941 | 44818 |
| 6.01 | 36.15 | 56.71 | 7.14 | 0.89 | 44.63 | 14.60 | 24.00 | 13.59 | 60.00 | 160834 | 47010 |
| 6.13 | 23.07 | 68.50 | 8.43 | 0.93 | 48.82 | 16.38 | 28.73 | 13.64 | 64.35 | 169989 | 50802 |
| 6.30 | 30.80 | 61.67 | 7.54 | 0.88 | 49.92 | 18.79 | 29.52 | 15.24 | 83.20 | 170026 | 55116 |
| 6.52 | 16.01 | 74.46 | 9.53 | 0.89 | 42.52 | 14.64 | 24.51 | 12.62 | 58.74 | 171648 | 51189 |
| 6.70 | 26.62 | 64.60 | 8.78 | 0.74 | 38.72 | 13.17 | 24.38 | 13.58 | 56.00 | 173312 | 46727 |
| 6.90 | 40.67 | 52.13 | 7.20 | 0.33 | 36.99 | 11.76 | 21.63 | 10.03 | 39.39 | 126078 | 38015 |
| 7.12 | 24.98 | 66.60 | 8.42 | 0.95 | 47.57 | 14.29 | 26.49 | 13.11 | 59.00 | 171095 | 54587 |
| 7.31 | 39.23 | 54.50 | 6.27 | 0.99 | 40.50 | 14.27 | 23.79 | 14.02 | 53.06 | 159653 | 45600 |
| 7.50 | 46.96 | 46.20 | 6.84 | 0.27 | 31.95 | 10.54 | 19.07 | 10.48 | 36.86 | 156843 | 43523 |
| 7.71 | 40.14 | 51.52 | 8.35 | 0.34 | 38.61 | 11.35 | 20.38 | 10.67 | 40.39 | 133480 | 37751 |
| 7.90 | 21.36 | 71.99 | 6.65 | 0.43 | 40.49 | 13.80 | 22.30 | 11.56 | 47.33 | 161497 | 48223 |
| 8.09 | 28.73 | 63.61 | 7.67 | 0.47 | 42.56 | 13.21 | 23.18 | 12.97 | 45.45 | 170303 | 47636 |
| 8.10 | 44.10 | 48.39 | 7.51 | 0.36 | 31.21 | 10.33 | 18.00 | 9.94 | 35.04 | 150686 | 40266 |
| 8.33 | 23.36 | 68.29 | 8.35 | 0.87 | 42.47 | 15.05 | 25.59 | 15.11 | 53.33 | 171038 | 50165 |
| 8.49 | 42.61 | 49.26 | 8.13 | 0.80 | 47.28 | 13.51 | 24.97 | 11.41 | 50.17 | 155540 | 46329 |
| 8.70 | 14.98 | 73.67 | 11.35 | 0.50 | 46.40 | 13.50 | 24.83 | 13.4 | 49.47 | 161646 | 45009 |
| 8.99 | 23.68 | 66.18 | 10.14 | 0.99 | 52.88 | 14.87 | 32.00 | 16.7 | 61.82 | 189026 | 56261 |
| 9.10 | 28.57 | 61.44 | 10.00 | 1.00 | 58.73 | 15.09 | 32.45 | 16.24 | 65.15 | 192972 | 57210 |
| 9.20 | 30.10 | 61.10 | 8.80 | 1.30 | 58.30 | 18.94 | 36.64 | 19.29 | 67.80 | 176538 | 55499 |
| 9.30 | 30.09 | 59.39 | 10.52 | 1.39 | 46.38 | 18.31 | 33.62 | 20.09 | 58.82 | 183334 | 51873 |
| 9.45 | 69.16 | 24.61 | 6.22 | 0.19 | 36.97 | 18.18 | 25.34 | 13.95 | 51.98 | 72673 | 16965 |
| 9.50 | 76.21 | 18.72 | 5.07 | 0.10 | 38.21 | 20.73 | 25.65 | 13.40 | 49.22 | 72336 | 16364 |
| 9.63 | 19.35 | 69.39 | 11.26 | 0.65 | 41.97 | 13.14 | 24.17 | 12.21 | 48.38 | 159643 | 44688 |
| 9.79 | 71.19 | 23.64 | 5.16 | 0.03 | 31.54 | 18.82 | 21.75 | 14.13 | 39.95 | 84269 | 17435 |
| 9.99 | 75.55 | 20.03 | 4.42 | 0.05 | 31.2 | 18.27 | 21.44 | 11.68 | 37.21 | 86544 | 17376 |
| 10.20 | 86.12 | 10.11 | 3.77 | 0.00 | 29.04 | 14.88 | 18.29 | 9.25 | 34.30 | 65305 | 16533 |
| 10.40 | 74.29 | 21.03 | 4.68 | 0.12 | 34.48 | 31.46 | 22.48 | 10.86 | 49.77 | 83895 | 18248 |
| 10.59 | 92.69 | 5.23 | 2.09 | 0.06 | 31.45 | 20.59 | 20.10 | 11.44 | 39.13 | 99053 | 22223 |

Table 4. Particle size distribution, organic carbon content and metal concentration values in RP-16 core. (mbsl: metres below sea level. Element concentrations in mg/kg).

| mbsl | % Sand | % Silt | % Clay | TOC | Cr | Cu | Ni | Pb | Zn | $Al_2O_3$ | $Fe_2O_3$ |
|---|---|---|---|---|---|---|---|---|---|---|---|
| 2.10 | 55.44 | 36.38 | 8.18 | 0.65 | 58.58 | 23.00 | 32.68 | 28.49 | 85.21 | 182912 | 70283 |
| 2.29 | 51.62 | 40.46 | 7.92 | 0.65 | 57.17 | 23.11 | 31.57 | 30.74 | 79.57 | 165893 | 51757 |
| 2.50 | 79.45 | 16.93 | 3.62 | 0.6 | 53.33 | 22.8 | 29.83 | 31.03 | 77.07 | 136998 | 40936 |
| 2.62 | 88.84 | 9.29 | 1.87 | 0.54 | 56.03 | 25.67 | 30.12 | 26.45 | 78.34 | 146078 | 34965 |
| 5.80 | 90.91 | 7.39 | 1.70 | 0.21 | 35.33 | 10.14 | 19.89 | 18.73 | 49.82 | 79822 | 16007 |
| 8.70 | 95.66 | 3.42 | 0.92 | 0.00 | 23.51 | 22.62 | 11.86 | 13.4 | 39.48 | 37798 | 8203 |
| 8.95 | 91.41 | 6.52 | 2.07 | 0.00 | 13.25 | 5.31 | 6.14 | 6.38 | 18.51 | 30830 | 6296 |
| 9.85 | 88.52 | 9.35 | 2.14 | 0.15 | 25.15 | 8.64 | 13.54 | 6.36 | 31.68 | 46870 | 11090 |
| 10.00 | 90.95 | 6.85 | 2.20 | 0.00 | 14.06 | 14.53 | 6.78 | 3.76 | 22.94 | 25911 | 7121 |
| 10.55 | 87.78 | 9.63 | 2.59 | 0.03 | 11.50 | 5.55 | 7.49 | 4.18 | 15.37 | 23871 | 5142 |
| 11.15 | 90.17 | 8.06 | 1.77 | 0.00 | 13.30 | 9.71 | 6.60 | 4.24 | 19.54 | 27007 | 5770 |
| 13.85 | 77.63 | 18.06 | 4.31 | 0.20 | 48.62 | 16.00 | 26.97 | 14.16 | 60.33 | 111122 | 33577 |
| 14.05 | 81.63 | 15.17 | 3.20 | 0.30 | 51.11 | 14.58 | 27.48 | 13.95 | 56.71 | 115433 | 37485 |
| 14.71 | 80.20 | 15.73 | 4.07 | 0.32 | 36.47 | 14.05 | 24.91 | 14.03 | 51.11 | 107349 | 32098 |
| 14.89 | 93.63 | 4.94 | 1.43 | 0.19 | 51.29 | 14.34 | 25.38 | 11.99 | 52.25 | 79556 | 23856 |
| 15.18 | 58.71 | 35.27 | 6.02 | 0.23 | 48.29 | 13.63 | 24.86 | 12.67 | 51.60 | 90230 | 25169 |
| 15.39 | 20.62 | 70.60 | 8.77 | 0.42 | 46.99 | 15.23 | 29.09 | 14.43 | 58.61 | 166767 | 53537 |
| 15.54 | 70.27 | 25.18 | 4.55 | 0.71 | 36.56 | 13.24 | 23.66 | 12.36 | 48.99 | 143289 | 38801 |
| 18.04 | 22.60 | 67.95 | 9.45 | 0.72 | 48.7 | 15.31 | 29.81 | 15.21 | 66.57 | 177508 | 56209 |

Table 5. Metal concentration in selected time slices (element concentrations in mg/Kg. Bold numbers indicated values used to calculate the backround).

| Age | Cr | Cu | Ni | Pb | Zn | $Al_2O_3$ | $Fe_2O_3$ total |
|---|---|---|---|---|---|---|---|
| **Core RP-15** | | | | | | | |
| ca.4000 calBP | 47.96 | 14.57 | 27.18 | 14.04 | 61.21 | 174755 | 42774 |
| **ca.6500 calBP** | **43.42** | **14.87** | **25.14** | **13.35** | **58.96** | **165791** | **47801** |
| ca.7000 calBP | 35.97 | 12.06 | 20.62 | 11.01 | 41.77 | 159153 | 45812 |
| ca. 7500 calBP | 44.88 | 14.28 | 25.28 | 13.26 | 51.75 | 163289 | 48247 |
| 8000-8500 calBP | 44.97 | 19.04 | 30.31 | 16.68 | 59.96 | 126220 | 35175 |
| ca. 9000 calBP | 31.45 | 20.59 | 20.10 | 11.44 | 39.13 | 99053 | 22223 |
| **Core RP-11b** | | | | | | | |
| surface | 41.30 | 21.53 | 28.54 | 22.60 | 80.84 | 176162 | 50760 |
| ca. 250 calBP | 46.10 | 18.39 | 31.11 | 16.52 | 66.40 | 178104 | 50876 |
| ca. 6500 calBP | 54.93 | 17.26 | 31.24 | 15.08 | 62.43 | 179837 | 52319 |
| ca. 7500 calBP | 34.92 | 10.67 | 20.23 | 9.34 | 43.96 | 86234 | 15905 |
| **Core RP-16** | | | | | | | |
| surface (1 m) | 58.58 | 23.00 | 32.68 | 28.49 | 85.21 | 182912 | 70283 |
| ca. 3000 calBP | 13.25 | 5.31 | 6.14 | 6.38 | 18.51 | 30830 | 6296 |
| ca. 8000-8500 calBP | 46.29 | 14.32 | 29.52 | 13.32 | 53.36 | 100779 | 31146 |
| ca. 9000 calBP | 48.70 | 15.31 | 29.81 | 15.21 | 66.57 | 177508 | 56209 |

Table 6. Contamination Factor (CF) and Contamination Degree (CD) in the selected time slices

| | | | CF | | | CD |
|---|---|---|---|---|---|---|
| **Age** | **Cr** | **Cu** | **Ni** | **Pb** | **Zn** | |
| **Core RP-15** | | | | | | |
| ca.4000 calBP | 1.10 | 0.98 | 1.08 | 1.05 | 1.04 | 5.25 |
| ca.6500 calBP | | | **background** | | | |
| ca.7000 calBP | 0.83 | 0.81 | 0.82 | 0.82 | 0.71 | 3.99 |
| ca. 7500 calBP | 1.03 | 0.96 | 1.01 | 0.99 | 0.88 | 4.87 |
| 8000-8500 calBP | 1.04 | 1.28 | 1.21 | 1.25 | 0.97 | 5.75 |
| ca. 9000 calBP | 0.72 | 1.39 | 0.80 | 0.86 | 0.66 | 4.43 |
| Core RP-11b | | | | | | |
| surface | 0.95 | 1.45 | 1.14 | 1.69 | 1.37 | 6.60 |
| ca. 250 calBP | 1.06 | 1.24 | 1.24 | 1.24 | 1.13 | 5.91 |
| ca. 6500 calBP | 1.26 | 1.16 | 1.24 | 1.13 | 1.06 | 5.85 |
| ca. 7500 calBP | 0.80 | 0.72 | 0.80 | 0.70 | 0.75 | 3.77 |
| Core RP-16 | | | | | | |
| surface (1 m) | 1.35 | 1.55 | 1.30 | 2.13 | 1.45 | 7.78 |
| ca. 3000 calBP | 0.31 | 0.36 | 0.24 | 0.48 | 0.31 | 1.70 |
| ca. 8000-8500 calBP | 1.07 | 0.97 | 1.03 | 1.00 | 0.90 | 4.97 |
| ca. 9000 calBP | 1.05 | 0.96 | 1.11 | 0.11 | 1.05 | 4.28 |

Table 7. Geoaccumulation Index ($I_{geo}$)in the selected time slices

| | $I_{geo}$ | | | | |
|---|---|---|---|---|---|
| **Age** | **Cr** | **Cu** | **Ni** | **Pb** | **Zn** |
| **Core RP-15** | | | | | |
| ca.4000 calBP | -0.41 | -0.48 | -0.68 | -0.73 | -0.75 |
| ca.6500 calBP | | | **background** | | |
| ca.7000 calBP | -0.82 | -0.91 | -0.88 | -0.88 | -1.10 |
| ca. 7500 calBP | -0.54 | -0.64 | -0.58 | -0.61 | -0.77 |
| 8000-8500 calBP | -0.56 | -0.23 | -0.33 | -0.29 | -0.65 |
| ca. 9000 calBP | -1.05 | -0.11 | -0.91 | -0.81 | -1.18 |
| **Core RP-11b** | | | | | |
| surface | -0.66 | -0.06 | -0.41 | 0.13 | -0.14 |
| ca. 250 calBP | -0.50 | -0.28 | -0.28 | -0.30 | -0.42 |
| ca. 6500 calBP | -0.25 | -0.37 | -0.27 | -0.41 | -0.50 |
| ca. 7500 calBP | -0.92 | -1.06 | -0.90 | -1.10 | -1.01 |
| **Core RP-16** | | | | | |
| surface (1 m) | -0.15 | 0.05 | -0.21 | 0.51 | -0.05 |
| ca. 3000 calBP | -2.30 | -2.07 | -2.62 | -1.65 | -2.26 |
| ca. 8000-8500 calBP | -0.51 | 0.64 | -0.54 | -0.59 | -0.73 |
| ca. 9000 calBP | -0.42 | -0.54 | -0.34 | -0.40 | -0.41 |

Table 8. Enrichment Factors (Al and Fe) in the selected time slices

| | $EF_{Al}$ | | | | | $EF_{Fe}$ | | | | |
|---|---|---|---|---|---|---|---|---|---|---|
| **Age** | **Cr** | **Cu** | **Ni** | **Pb** | **Zn** | **Cr** | **Cu** | **Ni** | **Pb** | **Zn** |
| **Core RP-15** | | | | | | | | | | |
| ca.4000 calBP | 1.05 | 0.93 | 1.03 | 0.10 | 0.99 | 1.23 | 1.10 | 1.21 | 1.18 | 1.16 |
| ca.6500 calBP | **background** | | | | | | | | | |
| ca.7000 calBP | 0.87 | 0.85 | 0.85 | 0.09 | 0.74 | 0.86 | 0.85 | 0.86 | 0.86 | 0.74 |
| ca. 7500 calBP | 1.06 | 0.98 | 1.02 | 0.10 | 0.89 | 1.03 | 0.95 | 1.00 | 0.98 | 0.87 |
| 8000-8500 calBP | 1.55 | 2.08 | 1.80 | 0.19 | 1.48 | 1.78 | 2.44 | 2.08 | 2.13 | 1.71 |
| ca. 9000 calBP | 1.22 | 2.32 | 1.34 | 0.14 | 1.11 | 1.56 | 2.99 | 1.72 | 1.84 | 1.43 |
| **Core RP-11b** | | | | | | | | | | |
| surface | 0.90 | 1.36 | 1.07 | 0.16 | 1.28 | 0.90 | 1.37 | 1.07 | 1.57 | 1.29 |
| ca. 250 calBP | 0.99 | 1.15 | 1.15 | 0.12 | 1.05 | 1.00 | 1.17 | 1.17 | 1.16 | 1.06 |
| ca. 6500 calBP | 1.17 | 1.08 | 1.15 | 0.10 | 0.98 | 1.17 | 1.08 | 1.15 | 1.05 | 0.98 |
| ca. 7500 calBP | 1.53 | 1.38 | 1.55 | 0.13 | 1.43 | 2.39 | 2.16 | 2.42 | 2.10 | 2.24 |
| **Core RP-16** | | | | | | | | | | |
| surface (1 m) | 1.23 | 1.40 | 1.18 | 0.19 | 1.31 | 0.92 | 1.05 | 0.88 | 1.45 | 0.98 |
| ca. 3000 calBP | 1.65 | 1.92 | 1.31 | 0.26 | 1.69 | 2.32 | 2.72 | 1.85 | 3.63 | 2.38 |
| ca. 8000-8500 calBP | 1.82 | 1.63 | 1.74 | 0.17 | 1.52 | 1.71 | 1.53 | 1.63 | 1.57 | 1.43 |
| ca. 9000 calBP | 1.05 | 0.96 | 1.11 | 0.11 | 1.05 | 0.95 | 0.88 | 1.01 | 0.97 | 0.96 |

Table 9. Pearson correlation matrix showing the coefficients of correlation among grain size fractions. TOC and heavy metal contents in the RP-15 core. n=40

| | **Sand** | **Silt** | **Clay** | **TOC** | **Cr** | **Cu** | **Ni** | **Pb** | **Zn** |
|---|---|---|---|---|---|---|---|---|---|
| **Sand** | 1 | | | | | | | | |
| **Silt** | -0.998 | 1 | | | | | | | |
| **Clay** | -0.850 | 0.820 | 1 | | | | | | |
| **TOC** | -0.744 | 0.744 | 0.613 | 1 | | | | | |
| **Cr** | -0.618 | 0.612 | 0.577 | 0.801 | 1 | | | | |
| **Cu** | 0.486 | -0.486 | -0.405 | -0.149 | -0.022 | 1 | | | |
| **Ni** | -0.452 | 0.439 | 0.501 | 0.777 | 0.889 | 0.228 | 1 | | |
| **Pb** | -0.341 | 0.327 | 0.418 | 0.680 | 0.709 | 0.219 | 0.897 | 1 | |
| **Zn** | -0.517 | 0.523 | 0.382 | 0.808 | 0.818 | 0.197 | 0.820 | 0.685 | 1 |

Table 10. Pearson correlation matrix showing the coefficients of correlation among grain size fractions. TOC and heavy metal contents in the RP-11b core. n=32

| | **Sand** | **Silt** | **Clay** | **TOC** | **Cr** | **Cu** | **Ni** | **Pb** | **Zn** |
|---|---|---|---|---|---|---|---|---|---|
| **Sand** | 1 | | | | | | | | |
| **Silt** | -0.995 | 1 | | | | | | | |
| **Clay** | -0.682 | 0.604 | 1 | | | | | | |
| **TOC** | -0.744 | 0.758 | 0.381 | 1 | | | | | |
| **Cr** | -0.770 | 0.767 | 0.519 | 0.605 | 1 | | | | |
| **Cu** | -0.728 | 0.715 | 0.568 | 0.625 | 0.639 | 1 | | | |
| **Ni** | -0.785 | 0.788 | 0.485 | 0.698 | 0.830 | 0.752 | 1 | | |
| **Pb** | -0.418 | 0.409 | 0.337 | 0.309 | 0.409 | 0.766 | 0.600 | 1 | |
| **Zn** | -0.665 | 0.660 | 0.464 | 0.543 | 0.604 | 0.864 | 0.685 | 0.850 | 1 |

Table 11. Pearson correlation matrix showing the coefficients of correlation among grain size fractions. TOC and heavy metal contents in the RP16 stratigraphic cross section. n=19

| | **Sand** | **Silt** | **Clay** | **TOC** | **Cr** | **Cu** | **Ni** | **Pb** | **Zn** |
|---|---|---|---|---|---|---|---|---|---|
| **Sand** | 1 | | | | | | | | |
| **Silt** | -0.999 | 1 | | | | | | | |
| **Clay** | -0.961 | 0.950 | 1 | | | | | | |
| **TOC** | -0.643 | 0.632 | 0.697 | 1 | | | | | |
| **Cr** | -0.498 | 0.488 | 0.556 | 0.764 | 1 | | | | |
| **Cu** | -0.225 | 0.215 | 0.289 | 0.576 | 0.690 | 1 | | | |
| **Ni** | -0.587 | 0.576 | 0.638 | 0.836 | 0.978 | 0.655 | 1 | | |
| **Pb** | -0.312 | 0.297 | 0.413 | 0.750 | 0.807 | 0.816 | 0.794 | 1 | |
| **Zn** | -0.498 | 0.484 | 0.575 | 0.837 | 0.954 | 0.809 | 0.954 | 0.920 | 1 |